ChemPubSoc Europe

DOI: 10.1002/open.201500224

Open Access ChemistryOPEN Communications

Rational Design of Dual Active Sites in a Single Protein Scaffold: A Case Study of Heme Protein in Myoglobin

Xiao-Gang Shu,[a] Ji-Hu Su,[b] Ke-Jie Du,[a] Yong You,[c] Shu-Qin Gao,[c] Ge-Bo Wen,[c] Xiangshi Tan,[d] and Ying-Wu Lin*[a, c]

Rational protein design has been proven to be a powerful tool for creating functional artificial proteins. Although many artificial metalloproteins with a single active site have been successfully created, those with dual active sites in a single protein scaffold are still relatively rare. In this study, we rationally designed dual active sites in a single heme protein scaffold, myoglobin (Mb), by retaining the native heme site and creating a copper-binding site remotely through a single mutation of Arg118 to His or Met. Isothermal titration calorimetry (ITC) and electron paramagnetic resonance (EPR) studies confirmed that a copper-binding site of [3-His] or [2-His-1-Met] motif was successfully created in the single mutant of R118H Mb and R118M Mb, respectively. UV/Vis kinetic spectroscopy and EPR studies further revealed that both the heme site and the designed copper site exhibited nitrite reductase activity. This study presents a new example for rational protein design with multiple active sites in a single protein scaffold, which also lays the groundwork for further investigation of the structure and function relationship of heme/non-heme proteins.

Metalloproteins with multiple active sites usually perform biological functions effectively. For example, in cytochrome *c* oxidase (C*c*O), heme *a* delivers electrons to the heme *a*3:Cu_B site, where O_2 is reduced to H_2O,[1] and in copper nitrite reductase (NIR), type-1 copper delivers electrons to type-2 copper, the site of nitrite binding and reduction.[2] Moreover, a di-heme enzyme, MauG, possesses two hemes *c* in distinct spin states with a long-range charge-resonance model.[3] It is thus attractive to create functional artificial proteins with multiple active sites for more efficient biocatalysis. Rational protein design has been proven to be a powerful tool, based on the scaffold of either natural proteins or de novo proteins.[4] Although many artificial metalloproteins with a single active site have been successfully created,[4] those with dual active sites in the same protein are still relatively rare. Based on a protein dimer, Roelfes and co-workers designed an artificial metalloenzyme with dual copper sites capable of catalyzing the Diels–Alder reaction.[5] Using domain swapping for horse heart myoglobin (Mb), Hirota and co-workers designed a heterodimeric protein with two different heme active sites, which exhibits distinct ligand binding properties.[6] These artificial metalloproteins were designed using two proteins by dimerization. Alternatively, Dutton and co-workers designed 4-helix bundles that can accommodate two heme groups or one heme and one other cofactor such as zinc *chlorin*.[7] Moreover, dual Fe–S clusters or metal-binding sites for Zn and Hg can be created in 3-helix bundles.[8] Therefore, development of other methods to design functional proteins with dual active sites in a single protein scaffold will broaden the variety of artificial enzymes. Note that although simply fusing two enzymes together might be a straightforward method,[9] chemical modifications as commonly used for fusion, as well as protein–protein interactions, should be considered to minimize the side effects on the active sites.

Due to the small size (153 amino acids) with a single heme group, the easy-to-produce Mb has been favored as a protein model for heme protein design.[10] By redesigning the heme active site, the O_2 carrier Mb has been converted successfully into various artificial enzymes.[4a,d–h,10–11] Copper (Cu_B) and iron (Fe_B) binding sites can also be designed close to the heme iron, mimicking the heteronuclear metal center in C*c*O and nitric oxide reductase (NOR), respectively.[12] With these advances, we are interested in design of dual active sites remote from each other using Mb as a model protein to create multiple metal centers in the same protein scaffold, which potentially produces artificial enzymes more efficient than those with a single active site.

To this end, we adopted a new approach of retaining the native heme and creating another metal-binding site remotely from the heme site (Figure 1). The previous experience of designing a Cu_B site in the heme pocket of Mb suggests that it is essential to create a metal-binding motif, such as a motif of three histidine,[3-His], as found for the type-2 copper site in NIR.[2] By a close inspection of the crystal structure of sperm

[a] X.-G. Shu, Dr. K.-J. Du, Prof. Dr. Y.-W. Lin
School of Chemistry and Chemical Engineering
University of South China Hengyang 421001 (P. R. China)
E-mail: linlinying@hotmail.com
ywlin@usc.edu.cn

[b] Dr. J.-H. Su
Department of Modern Physics
University of Science and Technology of China, Hefei 230026 (P. R. China)

[c] Y. You, S.-Q. Gao, Prof. Dr. . D. G.-B. Wen, Prof. Dr. Y.-W. Lin
Laboratory of Protein Structure and Function
University of South China, Hengyang 421001 (P. R. China)

[d] Prof. Dr. X. Tan
Department of Chemistry, Shanghai Key Lab of Chemical Biology for Protein Research & Institute of Biomedical Science
Fudan University, Shanghai 200433 (P. R. China)

Supporting information for this article can be found under http://dx.doi.org/10.1002/open.201500224.

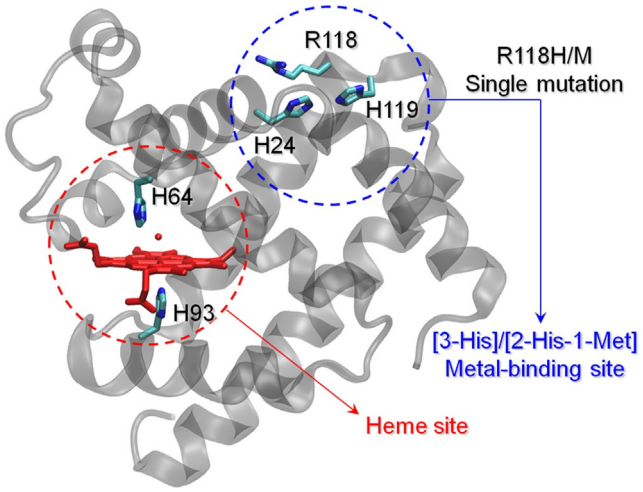

Figure 1. Design of dual active sites in a single protein scaffold of Mb.

whale Mb (PDB code 1JP6[13]), we found that a single mutation of Arg118 to His would create a [3-His] copper-binding motif, since the other two His residues (His24 and His119) are available in the native Mb with a proper conformation to form the motif (Figure 1). Similarly, mutation to Met would likely create a [2-His-1-Met] copper-binding site, as in the active site of peptidylglycine monooxygenase (PHM).[14]

The choice of Arg118 as the target for mutation to build the metal-binding motif was further supported by a crystallographic study of the F33Y Cu_BMb mutant in the presence of Cu^{II}.[15] The structure revealed that, when the protein crystal was soaked with an excess of copper ions (10 equiv $CuSO_4$), in addition to the copper in the designed Cu_B site, there were four other copper-binding sites in the crystal structure (Figure S1 in the Supporting Information). Notably, a copper (Cu_1, ~20 Å from the heme iron) is coordinated by both His24 (2.03 Å) and His119 (1.67 Å), as well as a water molecule (3.69 Å). We hypothesize that this Cu_1-binding site containing two His residues is more stable than the other three copper-binding sites on the protein surface. Moreover, the C_D atom of Arg118 is close to Cu_1 with a distance of 3.79 Å, suggesting that a His or Met introduced at this position may serve as an additional ligand for the copper. These observations encouraged us to construct both R118H Mb and R118M Mb single mutants.

R118H Mb and R118M Mb mutants were expressed and purified using the procedure reported previously.[12a] The protein was confirmed by matrix-assisted laser desorption time-of-fight (MALDI-TOF) mass spectrometry studies (Figure S2 in the Supporting Information). To investigate whether any copper binds to the designed metal-binding site, we performed isothermal titration calorimetry (ITC) studies for the two single mutants, with WT Mb as a control. Titration of Cu^{II} into the solution of WT Mb caused only a slight change in binding enthalpy. In contrast, major changes were observed when the Cu^{II} was titrated into a solution containing R118M Mb or R118H Mb under the same condition (Figure 2). These results strongly suggest that introducing the R118H or R118M mutation increases the Cu^{II}-binding significantly over that of WT Mb. To obtain quantitative information of the binding, we used a single-site binding model to fit the data, yielding a dissociation constant (K_d) value of ~81 and ~11 μM, and a stoichiometry of Cu^{II} to protein of 0.83 ± 0.31 and 1.02 ± 0.05, for R118M Mb and R118H Mb, respectively. Note that due to the limitation of ITC technique as well as data fitting, these results should be treated as approximate values. Moreover, slight changes in binding enthalpy were still observed for the two mutants with Cu^{II}/Mb ratio higher than 2 (Figure 2B,C), which suggests the existence of a weak binding site or nonspecific binding to the protein surface. The data fitting for WT Mb showed a larger K_d

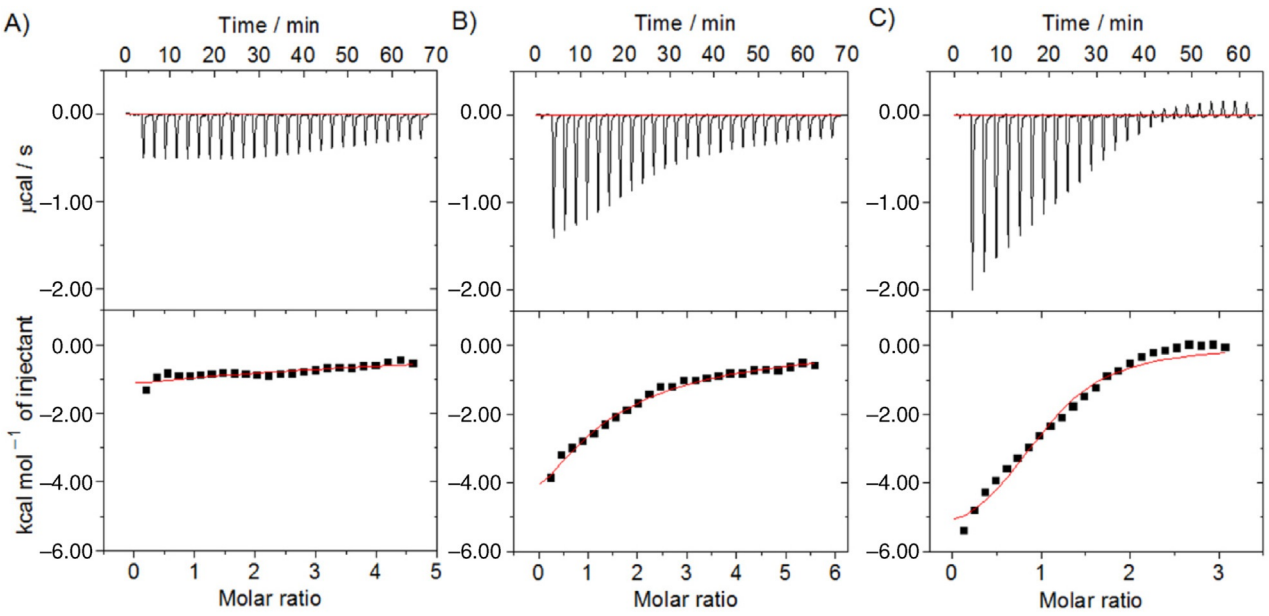

Figure 2. ITC data for titration of WT Mb (A), R118M Mb (B), and R118H Mb (C) with Cu^{II} at 25 °C. Top, raw data. Bottom, plot of integrated heats versus Cu^{II}/Mb ratio.

value of ~752 μM, with a stoichiometry of 1.73±0.28, likely due to the binding of Cu^{II} to other sites such as the Cu_2 site (Figure S1 in the Supporting Information). These results demonstrate that the [3-His] and [2-His-1-Met] copper-binding sites were successfully constructed in Mb by a single mutation, with both sites exhibiting an affinity for Cu^{II} much higher (~68- and ~9-fold, respectively) than that for WT Mb, although another weak binding site may also exist on the protein surface of the mutants.

To further confirm the Cu^{II} binding to the designed metal-binding site, we collected electron paramagnetic resonance (EPR) spectra. As shown in Figure 3A, the EPR spectra of R118H Mb and R118M Mb mutants in presence of 1 equiv Cu^{II} have features typical of the type-2 copper,[16] which are distinct from that for the free Cu^{II} in solution, indicating the binding of copper to protein. Although a similar spectrum was observed for Cu^{II}-WT Mb under the same conditions, shoulder peaks appeared in the parallel region, as indicated by arrows (Figure 3B). EPR simulation suggested that there are two copper-binding sites with a ratio of ~1:0.7 in WT Mb, whereas site-2 was not obvious for either Cu^{II}-R118M Mb or Cu^{II}-R118H Mb (Figure S3 in the Supporting Information and Table 1). It should be noted that although ITC studies suggested there were free Cu^{II} in WT Mb with 1 equiv Cu^{II} due to the large K_d value, the EPR spectrum collected at a much higher (~10-fold) concentration and lower temperature than the ITC studies showed copper binding to the protein. Meanwhile, a free Cu^{II} signal was indeed observed in EPR titration with excess Cu^{II} ions (Figure 4A). EPR titration further showed that additional Cu^{II} would bind to site-2 on the protein surface, and the signal intensity of site-1 with respect to site-2 is higher for the mutants than that for WT Mb (Figure 4B). These observations suggest that upon mutation of Arg118 in site-1, His118 or Met118 acts as an additional ligand for the copper, resulting in a higher copper binding affinity.

Note that Cu^{II}-R118M Mb has identical g values to the site-1 of Mb (Table 1), which suggests that coordination of Met118 causes no geometry alteration for the copper. This may be attributed to that fact that Met has the same side chain of C_{A-C} atoms to that of Arg, and the sulfur atom of Met118 is likely in

Table 1. Comparison of spin Hamiltonian parameters deduced from the simulation of the EPR spectra.

Copper-binding site	g_x	g_y	g_z
WT Mb (Site-1)	2.047	2.050	2.263
WT Mb (Site-2)	2.052	2.052	2.305
R118H Mb ([3-His])	2.047	2.048	2.250
R118M Mb ([2-His-1-Met])	2.047	2.050	2.263
PHM ([3-His])	2.043	2.070	2.263
PHM ([2-His-1-Met])	2.045	2.071	2.280
NIR (Type-2 Cu site)	2.076	2.076	2.358

Mb: myoglobin, PHM: peptidylglycine monooxygenase, NIR: nitrite reductase

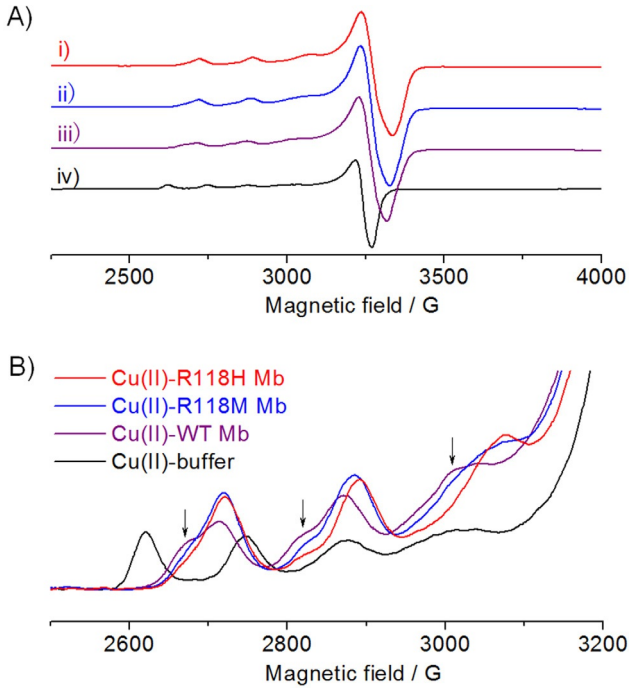

Figure 3. A) EPR spectra of R118H Mb (i), R118M Mb (ii), and WT Mb (iii) (0.3 mM) in the presence of 1 equiv Cu^{II} and free Cu^{II} in buffer (iv), collected at 30 K, 2 mW power, and 9.43 GHz. B) Expanded view comparison of the parallel hyperfine region of the spectra in (A).

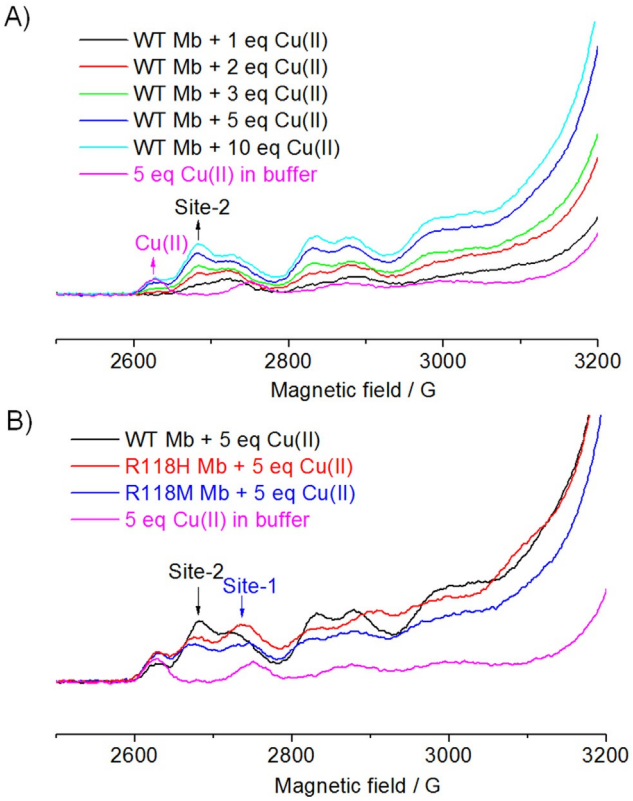

Figure 4. A) EPR spectra for Cu^{II} (1, 2, 3, 5, and 10 equiv) titration of WT Mb (0.18 mM) and 5 equiv free Cu^{II} in the same buffer solution (the arrow indicates the free Cu^{II} and Cu^{II} bound to site-2, respectively). B) EPR spectra comparison of R118H Mb, R118M Mb, and WT Mb in the presence of 5 equiv Cu^{II} under the same conditions (Cu^{II} binding sites are indicated by arrows).

a similar position of the C_D atom of Arg118, with a short distance favorable for direct coordination (Figure S1 in the Supporting Information). Interestingly, the Cu^{II}-R118H Mb has a *g* value slightly lower than that of Cu^{II}-R118M Mb, which is consistent with the prediction that metal-binding sites with more N donors have lower *g* values based on Peisach–Blumberg correlations.[17] These findings also agree with a recent study of Cu^{II} binding to engineered PHM mutants with a [3-His] or [2-His-1-Met] copper-binding site (Table 1).[14] Meanwhile, when compared with the type-2 copper site in native NIR from *Alcalogenes faecalis* (Table 1),[18] large differences in *g* values were observed for both Cu^{II}-R118H Mb and Cu^{II}-R118M Mb, indicating that the artificially constructed copper site in Mb does not identically reproduce the geometry of the type-2 copper in native NIR. These structural differences might have profound effects on the protein reactivity of nitrite reduction.

After confirming that Cu^{II} indeed binds to the single mutants of Mb, we then tested whether the copper site confers NIR activity, as it resembles the active site of native copper NIR,[2] albeit not identically. We performed an ascorbate–nitrite assay, which was demonstrated by Pecoraro and co-workers for testing the NIR activity of type-2 copper center designed in α-helical coiled coils.[19] In this assay, ascorbate acts as a sacrificial reductant for Cu^{II}, and the resultant Cu^{I}-bound protein catalytically reduces nitrite to NO. The oxidation of ascorbate was monitored by the decrease of its absorption at 265 nm (Figure 5A). Based on the changes of A_{265nm} as a function of time

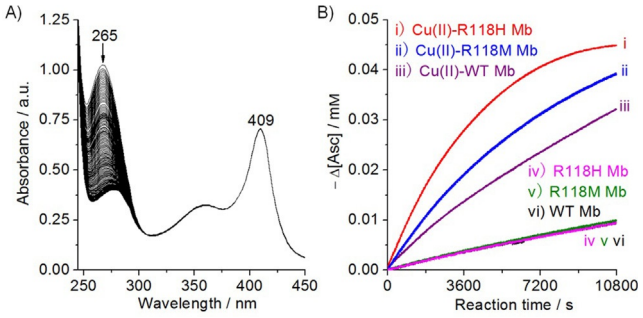

Figure 5. A) UV/Vis spectra of a solution of sodium ascorbate (45 μM) and $NaNO_2$ (5 mM) collected each minute, containing R118H Mb (5 μM) and Cu^{II} (5 μM). B) Decreases of [Asc^-] versus time in samples containing R118H Mb, R118M Mb, or WT Mb in the absence or presence of Cu^{II}.

(Figure 5B), the initial rate of ascorbate oxidation ($v_{ASC,Ox}$) for the first 2000 sec was calculated to be $(0.90\pm0.05)\times10^{-5}$ mM s^{-1} for Cu^{II}-R118H Mb. This value is 2.25- and 1.55-fold of that for Cu^{II}-WT Mb ($(0.40\pm0.02)\times10^{-5}$ mM s^{-1}) and Cu^{II}-R118M Mb ($(0.58\pm0.02)\times10^{-5}$ mM s^{-1}), respectively. These results suggest that the copper site in Mb with a higher copper affinity exhibits a higher NIR activity, presumably due to a higher occupancy of the copper site according to the ITC studies. The charge of the active site changed upon mutation of Arg118 might also affect the binding and reduction of nitrite. Note that Cu^{II} alone did not show catalytic activity in this assay, as confirmed in previous study.[19] In the absence of Cu^{II} ions, a low oxidation rate ($(0.10\pm0.01)\times10^{-5}$ mM s^{-1}) of ascorbate was observed for WT Mb and its mutants, which may be due to an auto-oxidation of ascorbate,[20] since the heme iron remained in the ferric state in these conditions, and no reaction occurred at the heme site. Additionally, the NO product in this essay was confirmed by addition of the headspace gas in the reaction cuvette for Cu^{II}-R118H Mb to deoxy WT Mb, which resulted in the formation of the NO-bound form, as shown in the UV/Vis spectrum (Figure S4 in the Supporting Information).

To verify that the heme site in the Cu^{II}-R118H Mb can also exhibit NIR activity, we increased the concentration of ascorbate to quickly reduce not only the Cu^{II}, but also the heme Fe^{III}. As shown in Figure 6A, the Soret band changed over time

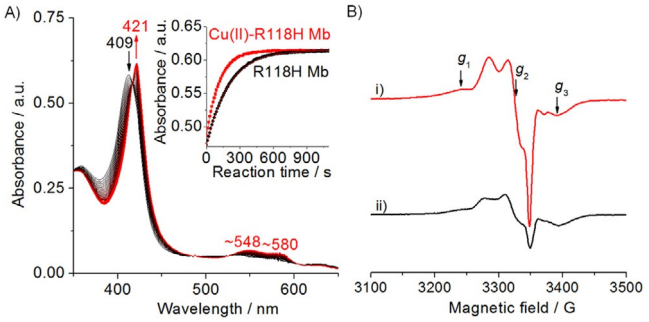

Figure 6. A) UV/Vis spectral changes for formation of NO–heme iron(II) complex upon nitrite (5 mM) reduction by Cu^{II}-R118H Mb (5 μM) with ascorbate (12 mM). Kinetic traces at 421 nm are shown as an inset. B) EPR spectra of nitrite reduction by R118H Mb (0.18 mM) in the presence (i) and absence (ii) of 1 equiv Cu^{II} for 5 min.

from 409 to 421 nm. Two visible bands appeared at ~548 and ~580 nm, indicating a conversion of the met form to the NO-bound ferrous form (NO–Fe^{2+}).[21] No observation of the ferrous heme in the reaction further suggested fast reduction of NO_2^- and binding of NO. With 1 equiv Cu^{II} added, the observed rate constant (k_{obs}) of formation of the NO–Fe^{2+} complex ($(8.73\pm0.05)\times10^{-3}$ s^{-1}) is ~1.7-fold higher than the protein alone ($(5.19\pm0.03)\times10^{-3}$ s^{-1}). A ~1.4- and ~1.1-fold k_{obs} was also observed for R118M Mb and WT Mb, respectively, upon Cu^{II} binding (Figure S5 in the Supporting Information). These results indicate that the NO produced at the Cu site may compete with NO_2^- and rapidly bind to the ferrous heme center. Since the NO produced at the heme site will also readily bind to the ferrous heme center in situ, we did not expect too much for the enhancement of k_{obs} contributed by the Cu site. Moreover, the NO product was confirmed by EPR studies (Figure 6B and inset of Figure S5 in the Supporting Information), which exhibited characteristic signals of a nitrosyl ferrous heme complex (g_1~2.078, g_2~2.027, g_3~1.988), similar to previous observations (g_1~2.08, g_2~2.01, g_3~1.98).[22] The enhanced intensity of the signals further indicates that both the Cu and heme sites are reactive.

In conclusion, we demonstrated that dual active sites can be designed in Mb by retaining the native heme site and creating a remote copper-binding site through a single mutation. This study presents a new example for rational protein design with multiple active sites in a single protein scaffold. In addition,

the NIR activity was demonstrated for both the heme and Cu sites, making it possible for this study to lay the groundwork for further investigation of the structure and function relationship of heme/non-heme proteins using the single protein scaffold, by redesigning not only the heme site, but also the Cu site such as introducing other metal ions.

Experimental Section

Experimental details, X-ray crystal structure of Cu^{II}-loaded F33Y Cu_BMb, [15] MALDI-TOF mass spectra, EPR simulation, and extra UV/Vis, EPR spectra are provided in the Supporting Information.

Acknowledgements

The authors gratefully thank Prof. Yi Lu of the University of Illinois at Urbana-Champaign, USA, for critical revising of the manuscript and helpful suggestions, and Dr. Yu Xiang of Tsinghua University, China, for performing MALDI-TOF mass spectrometry studies. EPR spectra were collected at the high magnetic field laboratory of the Chinese Academy of Science. This work was supported by the National Science Foundation of China (31370812, 21472027), Hunan Provincial Natural Science Foundation (2015JJ1012), Scientific Research Fund of Hunan Provincial Education Department (15A158, 13C817), and the Zhengxiang Scholar Program of the University of South China (Y.-W. Lin).

Keywords: electron paramagnetic resonance (EPR) · heme proteins · metal-binding site · nitrite reductase · protein design

[1] J. Liu, S. Chakraborty, P. Hosseinzadeh, Y. Yu, S. Tian, I. Petrik, A. Bhagi, Y. Lu, *Chem. Rev.* **2014**, *114*, 4366 – 4469.
[2] S. Suzuki, K. Kataoka, K. Yamaguchi, *Acc. Chem. Res.* **2000**, *33*, 728 – 735.
[3] J. Geng, I. Davis, A. Liu, *Angew. Chem. Int. Ed.* **2015**, *54*, 3692 – 3696; *Angew. Chem.* **2015**, *127*, 3763 – 3767.
[4] a) Y. Lu, N. Yeung, N. Sieracki, N. M. Marshall, *Nature* **2009**, *460*, 855 – 862; b) V. Nanda, R. L. Koder, *Nat. Chem.* **2010**, *2*, 15 – 24; c) P. A. Sontz, W. J. Song, F. A. Tezcan, *Curr. Opin. Chem. Biol.* **2014**, *19*, 42 – 49; d) I. D. Petrik, J. Liu, Y. Lu, *Curr. Opin. Chem. Biol.* **2014**, *19*, 67 – 75; e) M. Dürrenberger, T. R. Ward, *Curr. Opin. Chem. Biol.* **2014**, *19*, 99 – 106; f) K. Oohora, T. Hayashi, *Curr. Opin. Chem. Biol.* **2014**, *19*, 154 – 161; g) O. Shoji, Y. Watanabe, *J. Biol. Inorg. Chem.* **2014**, *19*, 529 – 539; h) C. Hu, S. I. Chan, E. B. Sawyer, Y. Yu, J. Wang, *Chem. Soc. Rev.* **2014**, *43*, 6498 – 6510.
[5] J. Bos, F. Fusetti, A. J. Driessen, G. Roelfes, *Angew. Chem. Int. Ed.* **2012**, *51*, 7472 – 7475; *Angew. Chem.* **2012**, *124*, 7590 – 7593.
[6] Y.-W. Lin, S. Nagao, M. Zhang, Y. Shomura, Y. Higuchi, S. Hirota, *Angew. Chem. Int. Ed.* **2015**, *54*, 511 – 515; *Angew. Chem.* **2015**, *127*, 521 – 525.
[7] T. A. Farid, G. Kodali, L. A. Solomon, B. R. Lichtenstein, M. M. Sheehan, B. A. Fry, C. Bialas, N. M. Ennist, J. A. Siedlecki, Z. Zhao, M. A. Stetz, K. G. Valentine, J. L. Anderson, A. J. Wand, B. M. Discher, C. C. Moser, P. L. Dutton, *Nat. Chem. Biol.* **2013**, *9*, 826 – 833.
[8] a) A. Roy, I. Sarrou, M. D. Vaughn, A. V. Astashkin, G. Ghirlanda, *Biochemistry* **2013**, *52*, 7586 – 7594; b) A. G. Tebo, V. L. Pecoraro, *Curr. Opin. Chem. Biol.* **2015**, *25*, 65 – 70.
[9] S. Schoffelen, J. C. M. van Hest, *Soft Matter* **2012**, *8*, 1736 – 1746.
[10] Y. Lin, J. Wang, Y. Lu, *Sci. China Chem.* **2014**, *57*, 346 – 355.
[11] a) J. Du, M. Sono, J. H. Dawson, *Coord. Chem. Rev.* **2011**, *255*, 700 – 716; b) Y.-W. Lin, C.-M. Nie, L.-F. Liao, *J. Mol. Model.* **2012**, *18*, 4409 – 4415; c) Y.-W. Lin, E. B. Sawyer, J. Wang, *Chem. Asian J.* **2013**, *8*, 2534 – 2544; d) Y.-B. Cai, X.-H. Li, J. Jing, J.-L. Zhang, *Metallomics* **2013**, *5*, 828 – 835; e) D. J. Sommer, M. D. Vaughn, G. Ghirlanda, *Chem. Br. Chem. Commun. (Camb.)* **2014**, *50*, 15852 – 15855; f) Y. Yu, C. Hu, X. Liu, I. D. Petrik, J. Wang, Y. Lu, *J. Am. Chem. Soc.* **2015**, *137*, 11570 – 11573; g) M. Bordeaux, V. Tyagi, R. Fasan, *Angew. Chem. Int. Ed.* **2015**, *54*, 1744 – 1748; *Angew. Chem.* **2015**, *127*, 1764 – 1768; h) J.-F. Du, W. Li, L. Li, G.-B. Wen, Y.-W. Lin, X. Tan, *ChemistryOpen* **2015**, *4*, 97 – 101; i) Y. Zhao, K.-J. Du, S.-Q. Gao, B. He, G.-B. Wen, X. Tan, Y.-W. Lin, *J. Inorg. Biochem.* **2016**, *156*, 113 – 121; j) Y. Morita, K. Oohora, A. Sawada, K. Doitomi, J. Ohbayashi, T. Kamachi, K. Yoshizawa, Y. Hisaeda, T. Hayashi, *Dalton Trans.* **2016**, *45*, 3277 – 3284.
[12] a) J. A. Sigman, B. C. Kwok, Y. Lu, *J. Am. Chem. Soc.* **2000**, *122*, 8192 – 8196; b) N. Yeung, Y.-W. Lin, Y.-G. Gao, X. Zhao, B. S. Russell, L. Lei, K. D. Miner, H. Robinson, Y. Lu, *Nature* **2009**, *462*, 1079 – 1082.
[13] P. Urayama, G. N. Phillips, Jr., S. M. Gruner, *Structure* **2002**, *10*, 51 – 60.
[14] S. Chauhan, C. D. Kline, M. Mayfield, N. J. Blackburn, *Biochemistry* **2014**, *53*, 1069 – 1080.
[15] K. D. Miner, A. Mukherjee, Y.-G. Gao, E. L. Null, I. D. Petrik, X. Zhao, N. Yeung, H. Robinson, Y. Lu, *Angew. Chem. Int. Ed.* **2012**, *51*, 5589 – 5592; *Angew. Chem.* **2012**, *124*, 5687 – 5690.
[16] T. D. Wilson, Y. Yu, Y. Lu, *Coord. Chem. Rev.* **2013**, *257*, 260 – 276.
[17] J. Peisach, W. E. Blumberg, *Arch. Biochem. Biophys.* **1974**, *165*, 691 – 708.
[18] M. Fittipaldi, H. J. Wijma, M. P. Verbeet, G. W. Canters, M. Huber, *Appl. Magn. Reson.* **2006**, *30*, 417 – 426.
[19] M. Tegoni, F. Yu, M. Bersellini, J. E. Penner-Hahn, V. L. Pecoraro, *Proc. Natl. Acad. Sci. USA* **2012**, *109*, 21234 – 21239.
[20] J. E. Fleming, K. Miyashita, S. C. Quay, K. G. Bensch, *Biochem. Biophys. Res. Commun.* **1983**, *115*, 531 – 535.
[21] J. Heinecke, P. C. Ford, *J. Am. Chem. Soc.* **2010**, *132*, 9240 – 9243.
[22] P. K. Witting, D. J. Douglas, A. G. Mauk, *J. Biol. Chem.* **2001**, *276*, 3991 – 3998.

Received: December 28, 2015
Published online on March 8, 2016

